

A-type Antiferromagnetic and C-type Orbital-Ordered State in LaMnO₃ Using Cooperative Jahn-Teller Phonons

Takashi Hotta, Seiji Yunoki, Matthias Mayr, and Elbio Dagotto

National High Magnetic Field Laboratory, Florida State University, Tallahassee, Florida 32306
(August 21, 2021)

The effect of Jahn-Teller phonons on the magnetic and orbital structure of LaMnO₃ is investigated using a combination of relaxation and Monte Carlo techniques on three-dimensional clusters of MnO₆ octahedra. In the physically relevant region of parameter space for LaMnO₃, and after including small corrections due to tilting effects, the A-type antiferromagnetic and C-type orbital structures were stabilized, in agreement with experiments.

PACS numbers: 75.30.Kz, 75.50.Ee, 75.10.-b, 75.15.-m

The theoretical understanding of manganese oxides is among the most challenging current areas of research in condensed matter physics.¹ Experimental studies of manganites have revealed a rich phase diagram originating from the competition between charge, spin, and orbital degrees of freedoms. A simple starting framework for Mn-oxide investigations is contained in the double-exchange (DE) ideas, where ferromagnetism induced by hole doping arises from the optimization of the hole kinetic energy.² In addition, recent results using the one-orbital model revealed a more complicated ground state, with phase separation tendencies strongly competing with ferromagnetism,³ leading to a potential explanation of the Colossal Magneto-Resistance effect.⁴

However, to understand the fine details of the phase diagram of manganites the one-orbital model is not sufficient since the highly nontrivial A-type spin antiferro (AF) and C-type orbital structures observed experimentally in the undoped material LaMnO₃⁵ cannot be properly addressed in such a simple context. Certainly two-orbital models are needed to consider the nontrivial state of undoped manganites. In this framework the two-band model without phonons has been studied before, and the importance of the strong Coulomb repulsion has been remarked for the appearance of the A-AF state.⁶⁻⁹ However, Coulombic approaches have presented conflicting results regarding the orbital order that coexists with the A-type spin state, with several approaches predicting G-type orbital order, which is not observed in practice. In addition, many experiments suggest that Jahn-Teller (JT) phonons are important in manganites and, thus, at present it is unclear whether the dominant interaction between electrons in Mn-oxides should be considered Coulombic or phonon mediated. For this reason it is important to analyze if a purely JT-phononic calculation is able to reproduce the experimental properties of undoped manganites, goal that provides the motivation for the present paper. The main result observed in this effort is that A-AF order, in combination with a C-type orbital arrangement, is indeed induced by JT-phonons in realistic parameter regions for LaMnO₃, namely large Hund-coupling between e_g-electrons and t_{2g}-spins, small

AF interaction between t_{2g}-spins, and strong electron-lattice coupling. This shows that JT-based calculations can lead to correct qualitative predictions for manganites, actually improving on purely Coulombic approaches in the orbital sector.

To carry out the calculations note that experiments have revealed an orbital structure tightly related to the JT-distortion of the MnO₆ octahedron. If each JT-distortion would occur independently, optimal orbitals can be determined by minimizing the kinetic and interaction energy of the e_g-electrons, as in models with only Coulomb interactions. However, oxygens are shared between adjacent MnO₆ octahedra, indicating that the JT-distortions occurs *cooperatively*. Particularly in the undoped situation, all MnO₆ octahedra exhibit JT-distortions, indicating that such a cooperative effect is important.¹⁰ Thus, in order to understand the magnetic and orbital structures of LaMnO₃, the electron and lattice systems must be optimized simultaneously. However, not much effort has been devoted to the microscopic treatment of the cooperative effect,¹¹ although the JT-effect in the Mn-oxides has been addressed by several groups.¹²⁻¹⁴ To remedy this situation, here a computational investigation of cooperative JT-phonons in manganites is carried out, focusing on the $n = 1$ density, where n is the electron number per site.

The motion of e_g-electrons tightly coupled to the localized t_{2g}-spins and the local distortions of the MnO₆ octahedra is described by

$$\begin{aligned}
 H = & - \sum_{\mathbf{i}\mathbf{a}\gamma\gamma'\sigma} t_{\gamma\gamma'}^{\mathbf{a}} c_{\mathbf{i}\gamma\sigma}^{\dagger} c_{\mathbf{i}+\mathbf{a}\gamma'\sigma} - J_{\text{H}} \sum_{\mathbf{i}\gamma\sigma\sigma'} \mathbf{S}_{\mathbf{i}} \cdot c_{\mathbf{i}\gamma\sigma}^{\dagger} \boldsymbol{\sigma}_{\sigma\sigma'} c_{\mathbf{i}\gamma\sigma'} \\
 & + \lambda \sum_{\mathbf{i}\sigma\gamma\gamma'} c_{\mathbf{i}\gamma\sigma}^{\dagger} (Q_{1\mathbf{i}}\sigma_0 + Q_{2\mathbf{i}}\sigma_1 + Q_{3\mathbf{i}}\sigma_3)_{\gamma\gamma'} c_{\mathbf{i}\gamma'\sigma} \\
 & + J' \sum_{(\mathbf{i},\mathbf{j})} \mathbf{S}_{\mathbf{i}} \cdot \mathbf{S}_{\mathbf{j}} + (1/2) \sum_{\mathbf{i}} (\beta Q_{1\mathbf{i}}^2 + Q_{2\mathbf{i}}^2 + Q_{3\mathbf{i}}^2), \quad (1)
 \end{aligned}$$

where $c_{\mathbf{i}\mathbf{a}\sigma}$ ($c_{\mathbf{i}b\sigma}$) is the annihilation operator for an e_g-electron with spin σ in the $d_{x^2-y^2}$ ($d_{3z^2-r^2}$) orbital at site \mathbf{i} . The vector connecting nearest-neighbor (NN) sites is \mathbf{a} , $t_{\gamma\gamma'}^{\mathbf{a}}$ is the hopping amplitude between γ - and γ' -orbitals connecting NN-sites along the \mathbf{a} -direction via

the oxygen $2p$ -orbital, J_H is the Hund coupling, \mathbf{S}_i the localized classical t_{2g} -spin normalized to $|\mathbf{S}_i| = 1$, and $\boldsymbol{\sigma} = (\sigma_1, \sigma_2, \sigma_3)$ are the Pauli matrices. The dimensionless electron-phonon coupling constant is λ , Q_{1i} denotes the dimensionless distortion for the breathing mode of the MnO_6 octahedron, Q_{2i} and Q_{3i} are, respectively, JT distortions for the $(x^2 - y^2)$ - and $(3z^2 - r^2)$ -type modes, and σ_0 is the unit matrix. J' is the AF-coupling between NN t_{2g} -spins, and β is a parameter to be defined below.

To account for the cooperative nature of the JT-phonons, the normal coordinates for distortions of the MnO_6 octahedron are written¹¹ as $Q_{1i} = (1/\sqrt{3})(L_{xi} + L_{yi} + L_{zi})$, $Q_{2i} = (1/\sqrt{2})(L_{xi} - L_{yi})$, and $Q_{3i} = (1/\sqrt{6})(2L_{zi} - L_{xi} - L_{yi})$, where L_{ai} denotes the distance between neighboring oxygens along the \mathbf{a} -direction, given by $L_{ai} = L_a + (u_i^a - u_{i-a}^a)$. Here, L_a is the length between Mn-ions along the \mathbf{a} -axis and u_i^a denotes the deviation of oxygen from the equilibrium position along the Mn-Mn bond in the \mathbf{a} -direction.¹⁵ In general, L_a can be different for each direction, depending on the bulk properties of the lattice. Since the present work focuses on the microscopic mechanism for A-AF formation in LaMnO_3 , the undistorted lattice with $L_x = L_y = L_z$ is treated first, and then corrections will be added. In the cubic undistorted lattice, the hopping amplitudes are given by $t_{aa}^x = -\sqrt{3}t_{ab}^x = -\sqrt{3}t_{ba}^x = 3t_{bb}^x = t$ for the \mathbf{x} -direction, $t_{aa}^y = \sqrt{3}t_{ab}^y = \sqrt{3}t_{ba}^y = 3t_{bb}^y = t$ for the \mathbf{y} -direction, and $t_{bb}^z = 4t/3$ with $t_{aa}^z = t_{ab}^z = t_{ba}^z = 0$ for the \mathbf{z} -direction. The energy unit is t . The parameter β is defined as $\beta = (\omega_{br}/\omega_{JT})^2$, where ω_{br} and ω_{JT} are the vibration energies for manganite breathing- and JT-modes, respectively, assuming that the reduced masses for those modes are equal. Using experimental results and band-calculation data for ω_{br} and ω_{JT} ,¹⁶ it can be shown that $\beta \approx 2$. However, the results presented here are basically unchanged as long as β is larger than unity.

To study Hamiltonian Eq. (1), two numerical techniques were here applied. One is the relaxation technique, in which the optimal positions of the oxygens are determined by minimizing the total energy. In this calculation, only the stretching mode for the octahedron, namely $u_i^a + u_{i-a}^a = 0$, is taken into account. Moreover, the relaxation has been performed for fixed structures of the t_{2g} -spins such as ferro (F), A-type AF (A-AF), C-type AF (C-AF), and G-type AF (G-AF), shown in Fig. 1(a). The advantage of this method is that the optimal orbital structure can be rapidly obtained on small clusters. However, the assumptions involved in the relaxation procedure should be checked with an independent method. Such a check is performed with the unbiased MC simulations used before by our group.¹⁴ The dominant magnetic and orbital structures are deduced from correlation functions. In the MC method, the clusters currently reachable are $2 \times 2 \times 2$, $4 \times 4 \times 2$, and $4 \times 4 \times 4$. In spite of this size limitation, arising from the large number of degrees of freedom in the problem, the available clusters are sufficient for our mostly qualitative purposes.

In addition, the remarkable agreement between MC and relaxation methods lead us to believe that our results are representative of the bulk limit.

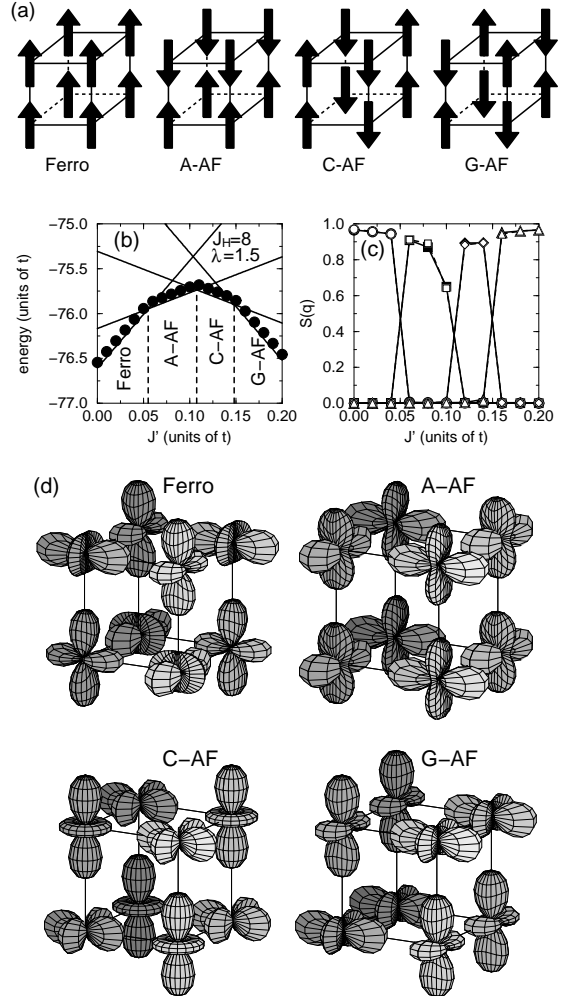


FIG. 1. (a) Magnetic structures in $2 \times 2 \times 2$ clusters. (b) Total energy as a function of J' on a $2 \times 2 \times 2$ lattice with $J_H = 8$ and $\lambda = 1.5$. The solid lines and circles indicate the relaxation and MC results, respectively. MC simulations have been performed at temperature $1/200$. (c) Spin correlation function $S(\mathbf{q})$ obtained by MC simulations as a function of J' , at $J_H = 8$ and $\lambda = 1.5$. Solid and open symbols denote the results in $4 \times 4 \times 2$ and $4 \times 4 \times 4$ clusters, respectively. Circles, squares, diamonds, and triangles indicates $S(\mathbf{q})$ for $\mathbf{q} = (0, 0, 0)$, $(\pi, 0, 0)$, $(\pi, \pi, 0)$, and (π, π, π) , respectively. (d) Optimized orbital structure for each magnetic structure.

In Fig. 1(b), the mean-energy is presented as a function of J' for $J_H = 8$ and $\lambda = 1.5$, on a $2 \times 2 \times 2$ cluster with open boundary conditions. The solid lines and symbols indicate the results obtained with the relaxation technique and MC simulations, respectively. The agreement is excellent, showing that the relaxation method is accurate. The small deviations between the results of

the two techniques are caused by temperature effects. As intuitively expected, with increasing J' the optimal magnetic structure changes from ferro- to antiferromagnetic, and this occurs in the order $F \rightarrow A\text{-AF} \rightarrow C\text{-AF} \rightarrow G\text{-AF}$. To check size effects, the t_{2g} -spin correlation function $S(\mathbf{q})$ was calculated also in $4 \times 4 \times 2$ and $4 \times 4 \times 4$ clusters, where $S(\mathbf{q}) = (1/N) \sum_{i,j} e^{-i\mathbf{q} \cdot (\mathbf{i}-\mathbf{j})} \langle \mathbf{S}_i \cdot \mathbf{S}_j \rangle$, N is the number of sites, and $\langle \dots \rangle$ indicates the thermal average value. As shown in Fig. 1(c), with increasing J' the dominant correlation changes in the order of $\mathbf{q} = (0, 0, 0)$, $(\pi, 0, 0)$, $(\pi, \pi, 0)$, and (π, π, π) . The values of J' at which the spin structures changes agree well with those in Fig. 1(b).

The shape of the occupied orbital arrangement with the lowest energy for each magnetic structure is in Fig. 1(d). For the F-case, the G-type orbital structure is naively expected, but actually a more complicated orbital structure is stabilized, indicating the importance of the cooperative treatment for JT-phonons. For the A-AF state,¹⁷ only the C-type structure is depicted, but the G-type structure, obtained by a $\pi/2$ -rotation of the upper x - y plane of the C-type state, was found to have *exactly* the same energy. Small corrections will remove this degeneracy in favor of the C-type as described below. For C- and G-AF, the obtained orbital structures are G- and C-types, respectively. Although the same change of the magnetic structure due to J' was already reported in the electronic model with purely Coulomb interactions,⁹ the orbital structures in those previous calculations were G-, G-, A-, and A-type for the F-, A-AF, C-AF, and G-AF spin states, respectively. Note that for the A-AF state, of relevance for the undoped manganites, the G-type order was obtained,⁹ although in another treatment for the Coulomb interaction, the C- and G-type structures were found to be degenerate,⁷ as in our calculation.

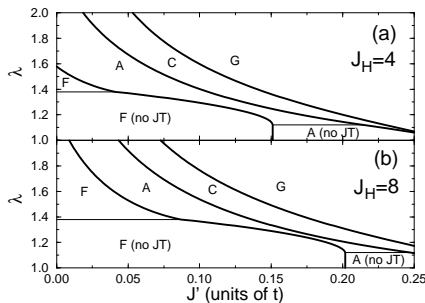


FIG. 2. Magnetic phase diagram on the (J', λ) plane for (a) $J_H = 4$ and (b) 8 (relaxation method). Below the thin solid lines in the F and A-AF regions, the JT-distortion disappears, suggesting that the system becomes metallic.

In Figs. 2 (a) and (b), the phase diagrams on the (J', λ) -plane are shown for $J_H = 4$ and 8, respectively. The curves are drawn by the relaxation method. As expected, the F-region becomes wider with increasing J_H . When λ is increased at fixed J_H , the magnetic structure changes from $F \rightarrow A\text{-AF} \rightarrow C\text{-AF} \rightarrow G\text{-AF}$. This tendency is qualitatively understood if the two-site problem is consid-

ered in the limit $J_H \gg 1$ and $E_{JT} \gg 1$, where E_{JT} is the static JT-energy given by $E_{JT} = \lambda^2/2$. The energy-gain due to the second-order hopping process of e_g -electrons is roughly $\delta E_{AF} \sim 1/J_H$ and $\delta E_F \sim 1/E_{JT}$ for AF- and F-spin pairs, respectively. Increasing E_{JT} , δE_F decreases, indicating the relative stabilization of the AF-phase. In our phase diagram, the A-AF phase appears for $\lambda \gtrsim 1.1$ and $J' \lesssim 0.15$. This region does not depend much on J_H , as long as $J_H \gg 1$. Although λ seems to be large, it is realistic from an experimental viewpoint: E_{JT} is 0.25eV from photoemission experiments¹⁸ and t is estimated as $0.2 \sim 0.5\text{eV}$,¹⁹ leading to $1 \lesssim \lambda \lesssim 1.6$. As for J' , it is estimated as $0.02 \lesssim J' \lesssim 0.1$.^{8,20} Thus, the location in parameter-space of the A-AF state found here is reasonable when compared with experimental results for LaMnO_3 .

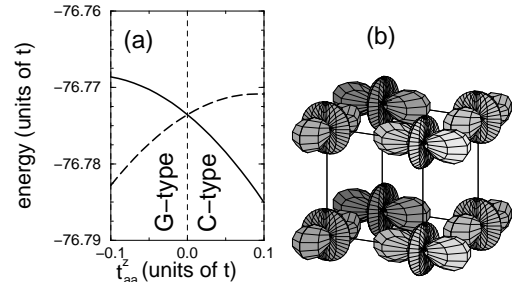


FIG. 3. (a) Total energy as a function of t_{aa}^z on the $2 \times 2 \times 2$ lattice with $L_x = L_y > L_z$ for $J_H = 8$, $\lambda = 1.6$ and $J' = 0.05$ (relaxation method). The solid and dashed curves denote the C- and G-orbital states, respectively. (b) Orbital structure in the A-AF phase for $t_{aa}^z = 0^+$ and $L_x = L_y > L_z$. These shapes are very close to purely $3x^2 - r^2$ and $3y^2 - r^2$ types.

Let us now focus on the orbital structure in the A-AF phase. In the cubic lattice studied thus far, the C- and G-type orbital structures are degenerate, and it is unclear whether the orbital pattern in the x - y plane corresponds to the alternation of $3x^2 - r^2$ and $3y^2 - r^2$ orbitals observed in experiments.⁵ To remedy the situation, some empirical facts observed in manganites become important: (i) The MnO_6 octahedra are slightly tilted from each other, leading to modifications in the hopping matrix. Among these modifications, the generation of a non-zero value for t_{aa}^z is important. (ii) The lattice is not cubic, but the relation $L_x \approx L_y > L_z$ holds. From experimental results,⁵ these numbers are estimated as $L_x = L_y = 4.12\text{\AA}$ and $L_z = 3.92\text{\AA}$, indicating that the distortion with Q_3 -symmetry occurs spontaneously. Note that the hopping amplitude and J' along the z -axis are different from those in the x - y plane due to this distortion. Motivated by these observations, the energies for C- and G-type orbital structures were recalculated including this time a nonzero value for t_{aa}^z in the magnetic A-AF state (see Fig. 3(a)). In the real material, it can be shown based on symmetry considerations that the tilting of the MnO_6 octahedra will always lead to a *positive* value for t_{aa}^z . Then, the results of Fig. 3(a) suggest that the C-type

orbital structure should be stabilized in the real materials, and the explicit shape of the occupied orbitals is shown in Fig. 3(b). The experimentally relevant C-type structure with the approximate alternation of $3x^2 - r^2$ and $3y^2 - r^2$ orbitals is indeed successfully obtained by this procedure. Although the octahedron tilting actually leads to a change of all hopping amplitudes, effect not including in this work, the present analysis is sufficient to show that the C-type orbital structure is stabilized in the A-AF magnetic phase when t_{aa}^z is a small positive number,²¹ as it occurs in the real materials.

In this work the Coulomb interactions (intra-orbital Coulomb U , inter-orbital Coulomb U' , and inter-orbital exchange J) have been neglected. For Mn-oxides, they are estimated as $U = 7\text{eV}$, $J = 2\text{eV}$, and $U' = 5\text{eV}$,⁸ which are large compared to t . However, the result for the optimized distortion described in this paper, obtained without the Coulomb interactions, is not expected to change since the energy gain due to the JT-distortion is maximized when a single e_g -electron is present per site. This is essentially the same effect as produced by a short-range repulsion. In fact, it has been checked explicitly by using the Exact Diagonalization method that the JT- and breathing-distortions are not changed by U' on a 2×2 cluster using the F-state in which U and J can be neglected. In addition, the MC simulations show that the probability of double occupancy of a single orbital is negligible where the A-type spin, C-type orbital state is stable.²² Based on all these observations, it is believed that the effect of the Coulomb interaction is not crucial for the appearance of the A-AF state with the proper orbital order. Another way to rationalize this result is that the integration of the JT-phonons at large λ will likely induce Coulombic interactions dynamically.

Finally, let us briefly discuss transitions induced by the application of external magnetic fields on undoped manganites. When the A-AF state is stabilized, the energy difference (per site) obtained in our study between the A-AF and F states is about $t/100$. As a consequence, magnetic fields of $20 \sim 50\text{T}$ could drive the transition from A-AF to F order accompanied by a change of orbital structure, interesting effect which may be observed in present magnetic field facilities.

Summarizing, using numerical techniques at $n = 1$ it has been shown that the A-AF state is stable in models with JT-phonons, using coupling values physically reasonable for LaMnO_3 . Our results indicate that it is not necessary to include large Coulombic interactions in the calculations to reproduce experimental results for the manganites. Considering the small but important effect of the octahedra tilting of the real materials, the C-type orbital structure (with the alternation pattern of $3x^2 - r^2$ and $3y^2 - r^2$ orbitals) has been successfully reproduced for the A-AF phase in this context.

T.H. thanks Y. Takada and H. Koizumi for enlightening discussion. T.H. is supported from the Ministry of

Education, Science, Sports, and Culture of Japan. E.D. is supported by grant NSF-DMR-9814350.

-
- ¹ Y. Tokura *et al.*, J. Appl. Phys. **79**, 5288 (1996); A. P. Ramirez, J. Phys.: Condens. Matter **9**, 8171 (1997).
² C. Zener, Phys. Rev. **82**, 403 (1951).
³ S. Yunoki *et al.*, Phys. Rev. Lett. **80**, 845 (1998).
⁴ A. Moreo *et al.*, Science **283**, 2034 (1999).
⁵ E. O. Wallan and W. C. Koeler, Phys. Rev. **100**, 545 (1955); G. Matsumoto, J. Phys. Soc. Jpn. **29**, 606 (1970). The C-type orbital structure has been recently confirmed with the use of high resolution X-ray diffraction technique (Y. Murakami *et al.*, Phys. Rev. Lett. **81**, 582 (1998)).
⁶ K. I. Kugel and D. I. Khomskii, Usp. Fiz. Nauk. **136**, 621 (1981)[Sov. Phys. USP. **25**, 231 (1982)]; W. Koshibae *et al.*, J. Phys. Soc. Jpn. **66**, 957 (1997); R. Shiina *et al.*, J. Phys. Soc. Jpn. **68**, 3159 (1997); L. F. Feiner and A. M. Oleś, Phys. Rev. **B59**, 3295 (1999); J. van den Brink *et al.*, Phys. Rev. **B59**, 6795 (1999).
⁷ T. Mizokawa and A. Fujimori, Phys. Rev. **B51**, 12880 (1995); *ibid* **54**, 5368 (1996).
⁸ S. Ishihara *et al.*, Phys. Rev. **B55**, 8280 (1997).
⁹ R. Maehzono *et al.*, Phys. Rev. **B57**, R13993 (1998).
¹⁰ J. Kanamori, J. Appl. Phys. **31**, S14 (1960).
¹¹ P. B. Allen and Vasili Perebeinos, cond-mat/9811250 and references therein.
¹² D. Feinberg *et al.*, Phys. Rev. **B57**, R5583 (1998).
¹³ H. Koizumi *et al.*, Phys. Rev. Lett. **80**, 4518 (1998).
¹⁴ S. Yunoki *et al.*, Phys. Rev. Lett. **81**, 5612 (1998).
¹⁵ In this work, the buckling and rotational modes of MnO_6 octahedron are not explicitly included.
¹⁶ M. N. Iliev *et al.*, Phys. Rev. **B57**, 2872 (1998).
¹⁷ In the A-type state there exists an additional triplet degeneracy due to the cubic symmetry for each magnetic structure: If axes are changed cyclically ($x \rightarrow y, y \rightarrow z, z \rightarrow x$), the optimized orbital structure is also transformed by this cyclic change, but the energy is invariant. Then, the magnetic and orbital structure in LaMnO_3 occurs through a *spontaneous* symmetry breaking process.
¹⁸ D. S. Dessau and Z.-X. Shen, in *Colossal Magnetoresistance Oxides*, ed. Y. Tokura, Gordon & Breach, Monographs in Cond. Matt. Science (1999).
¹⁹ A. E. Bacquet *et al.*, Phys. Rev. **B46**, 3771 (1992); T. Arima *et al.*, Phys. Rev. **B48**, 17006 (1993); T. Saito *et al.*, Phys. Rev. **B51**, 13942 (1995).
²⁰ T. G. Perring *et al.*, Phys. Rev. Lett. **78**, 3197 (1997).
²¹ It can be shown that this mechanism to stabilize the C-type structure works also for the purely electronic model in the Hartree-Fock approximation.
²² If the Coulomb interaction is included, it is expected that the A-AF state will be stabilized at smaller λ improving the comparison of our results with experiments (see P. Benedetti and R. Zeyher, Phys. Rev. **B59**, 9923 (1999)).